CHARACTERIZATION AND ADSORPTION PROPERTIES OF *HYPERICUM PERFORATUM* L. FOR THE REMOVAL OF Cu^{2+} IONS FROM AQUEOUS SOLUTIONS

LIDIA IVANOVA, PAUNKA VASSILEVA and ALBENA DETCHEVA

Bulgarian Academy of Sciences, Institute of General and Inorganic Chemistry,
Acad. Georgi Bonchev Str., Bl. 11, 1113, Sofia, Bulgaria
✉ *Corresponding author: Lidia Ivanova, lidia@svr.igic.bas.bg*

The objective of the present study is the characterization of an adsorbent plant material based on *Hypericum perforatum* L. and the investigation of its feasibility for the removal of Cu^{2+} ions from aqueous solutions. XRD, TGA, FTIR, SEM and low-temperature nitrogen adsorption were used for the analytical characterization of the material. Particle size distribution and slurry pH of the investigated material were also determined. The effect of contact time, solution acidity and initial metal concentration on the adsorption of Cu(II) ions was studied by means of the batch method. Desorption studies have also been performed. Equilibrium experimental data were fitted to the linear Langmuir, Freundlich and Dubinin-Radushkevich isotherm models. The maximum adsorption capacity was calculated and it was concluded that the material could be used as an effective biosorbent for the removal of copper ions from aqueous media.

Keywords: *Hypericum perforatum* L., characterization, adsorption, equilibrium, copper ions

INTRODUCTION

The search for new technologies to remove metals from wastewaters has directed attention to biosorption. It is a good alternative compared with conventional wastewater treatment techniques. Its major advantages are its low cost, high efficiency, minimization of chemical or biological sludge, and the possibility to regenerate the biosorbents and to recover the metals. Plant materials, being economic and ecofriendly due to their unique chemical composition and abundant availability, are frequently used as biosorbents.[1]

It has been proved[2,3] that lignocellulosics have ion-exchange capacity and general sorptive characteristics, which are derived from their constituent polymers and structure. The polymers include extractives, cellulose, hemicelluloses, pectin, lignin and protein. Biosorption of heavy metal ions can take place *via* several mechanisms, including ion exchange, complexation, coordination, chelating, physical adsorption *etc*.[4,5] The degree and rate of biosorption depend on the properties of metal ions, operating conditions, as well as the physical and surface properties of the biosorbent used.[6,7]

On the other hand, copper and its compounds are widely used at an industrial level and there are many potential sources of copper pollution.[8] Although copper is regarded as an essential element at low concentrations, it becomes toxic at higher concentrations and therefore is classified in the second group of toxicity of metal ions.[9] The continued intake of copper by human beings leads to many negative effects on their health.[8,10] Thus, being a threat to living organisms and especially for humans, copper has to be removed from industrial wastewaters before discharging them into the environment.

Hypericum perforatum L., known as St. John's wort, is a flowering plant spread in temperate regions worldwide as a cosmopolitan invasive weed. It is also grown commercially for use in herbalism and traditional medicine. No data concerning the biosorption of copper ions on *Hypericum perforatum* L. have been reported in the literature so far.

The present study investigates the utilization of a plant material based on *Hypericum perforatum* L. (denoted as HP) as biosorbent for

Cu^{2+} ions from aqueous solutions. HP is characterized in terms of mineralogical and chemical composition, grain size distribution, thermal behaviour, slurry pH, and texture parameters. The estimation of the optimal parameters influencing Cu(II) removal, such as contact time, solution acidity, temperature and initial metal concentration, was performed by means of the batch method. The possibility of regenerating the used biosorbent was also studied.

EXPERIMENTAL
Materials and methods
The commercially available fresh leaves and blossoms of *Hypericum perforatum* L. (denoted as HP) were washed several times with distilled water to remove surface-adhered and water-soluble particles, and dried at 60 °C in an electric oven for 48 h. The material was then milled in an electric grinder. No other physical or chemical treatment was performed on the material thus obtained.

The grain size distribution was determined on a Dynamic Image Analyzer Camsizer XT, X-Dry (Retsch Technology, Germany). For pH determination, sample suspensions (0.5 g of sample in 50 mL of deionized water) were prepared in stoppered 100-mL glass bottles. The mixtures were stirred for 24 h on a mechanical stirrer and after filtration, the pH values of the aqueous solutions were measured on a pH meter model 211, Hanna Instruments (Germany).

X-ray diffraction (XRD) patterns were obtained on a D8 Advance System from Bruker Inc. (Germany), using CuKα radiation (40 kV and 40 mA; λ = 1.5404 nm).

Moisture and ignition losses were measured by differential thermal analysis (DTA), and thermogravimetric analysis (TGA). DTA was performed on a Setaram Labsys Evo 1600 system, in the temperature range from room temperature up to 700 °C, at a heating rate of 10 °C/min in air atmosphere.

The Fourier transform infrared (FTIR) spectra were measured on a Thermo Nicolet 6700 FTIR spectrometer. Spectra were collected in the mid-infrared region (4000-400 cm^{-1}). The samples were prepared by the standard KBr pellet method.

The surface morphology of the biosorbent was observed on a scanning electron microscope (SEM) – a Tescan Lyra I XMU FIB SEM.

The porous structure of the studied material was investigated by low-temperature (-196 °C) nitrogen adsorption, using Quantachrome Nova 1200 apparatus (Quantachrome Instruments, USA). Before nitrogen adsorption, the samples were degassed at 80 °C for 3 h. The specific surface area was calculated on the basis of the Brunauer–Emmett–Teller (BET) equation; the pore size distribution was calculated according to the Barrett–Joyner–Halenda (BJH) method. The total pore volume was estimated in accordance with the rule of Gurvich at a relative pressure of 0.99.

Adsorption studies
Batch experiments were carried out to determine the adsorption properties of the plant material. Experiments were performed using stoppered 50-mL Erlenmeyer flasks containing about 0.2 g of sample and 20 mL of aqueous solution of Cu^{2+} ions. The mixture was shaken at room temperature (20 °C) by an automatic shaker. The initial solution pH was adjusted using 0.1 M HCl or 0.1 M NaOH. After the experiment, the biomaterial was removed by filtration through a Millipore filter (0.2 μm). The initial and equilibrium copper concentrations were determined by inductively coupled plasma optical emission spectrometry (ICP-OES) on a Prodigy 7 ICP-OES spectrometer (Teledyne Leeman Labs, USA).

The amount of adsorbed copper ions Qe was calculated using the following relationship:

$$Qe = (Co - Ce) * V/m \qquad (1)$$

where Co = initial concentration (mg L^{-1}), Ce = equilibrium concentration (mg L^{-1}), m = mass of adsorbent (g), and V = solution volume (L).

Deionized water and analytical grade reagents were used throughout. Working standard solutions of Cu^{2+} ions with concentrations of 50-500 mg L^{-1} were prepared by stepwise dilution of a stock solution with the concentration of 1 g Cu L^{-1} (CuCl$_2$ in H$_2$O), *Titrisol*® Merck (Darmstadt, Germany).

RESULTS AND DISCUSSION
Sample characterization
After sample pretreatment, the resulting grain size distribution was found to be at a maximum of about 100 ìm average particle size and more than 90% of the particles were below 160 μm. From the grain size distribution data, we suppose that the sample pretreatment ensures the representativeness and the homogeneity of the investigated material for the following experiments and measurements.

The XRD pattern of the sample HP is presented in Figure 1. The peak at around 22° 2θ is assigned to the crystalline form of cellulose I.[11,12] The range between 15° and 25° 2θ corresponds to amorphous phases of lignin, hemicelluloses and cellulose.[13-15]

The thermal behaviour of HP is presented in Figure 2. It is seen that, during the pyrolysis process, the phases containing different hydrocarbon compounds are removed, leaving a solid carbon-containing residue. The first region (20 to 100 °C) depicts the separation of moisture and adsorbed water. This region is not clearly distinguished, owing to the preliminary drying of

the HP sample at 60 °C in an electric oven for 48 h. The second region (100 to 200 °C) is related to the evaporation of highly volatile compounds present in the sample. The shape of the third region (200 to 400 °C) corresponds to the thermal degradation of hemicelluloses, cellulose and some lignin fractions. The region above 400 °C is assigned to the decomposition of the rest of lignin.[11,16]

Knowledge of the textural parameters of the sorbents is important for understanding their potential in the adsorption process. Figure 3 shows the nitrogen adsorption–desorption isotherm and pore size distribution curve of the studied biosorbent. It exhibits a type IV isotherm, with an H3 type hysteresis loop, namely, typical hysteresis loops of mesoporous materials. A relatively narrow pore size distribution of about 4 nm can be observed in the Barrett–Joyner–Halenda pore size distribution curve, which further demonstrates the existence of mesopores. The specific surface area of the studied material is 0.8 m^2g^{-1}, with a mean pore volume of 0.001 cm^3

g^{-1}. The slurry pH values indicate that the HP sample exhibits acidic reaction (pH about 4.6).

Adsorption studies
Effect of pH

The pH of the aqueous solution has a significant impact on the adsorption of metal ions on the adsorbents. The adsorption efficiency of the studied material as a function of the initial solution pH is presented in Figure 4. As expected, the removal of copper ions strongly depends on the acidity of the initial solutions. Upon increasing the pH value, the amount of adsorbed ions increased and the optimum pH range was found to be about 4.0. The adsorption can be explained on the basis of competitive adsorption of H^+ and OH^- ions, on the one hand, and the copper ions on the other. The removal of Cu(II) ions could, therefore, be the combined result of ion exchange and surface complexation phenomena occurring on the surface of the investigated material.
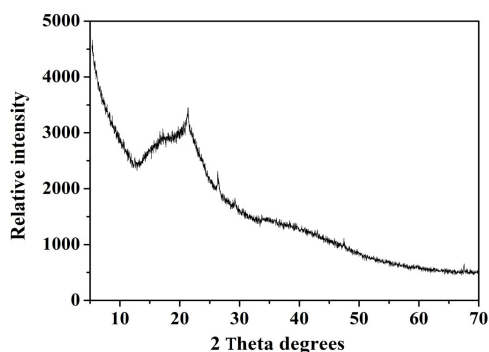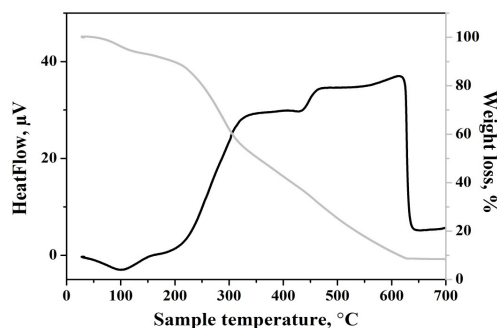

Figure 1: X-ray diffraction pattern for HP

Figure 2: Differential thermal analysis and thermogravimetric analysis curves for HP
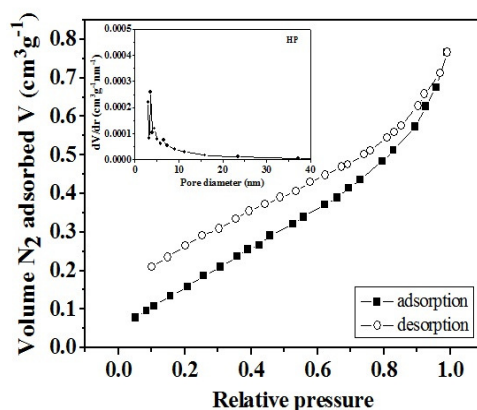

Figure 3: Nitrogen adsorption–desorption isotherm and pore size distribution of HP
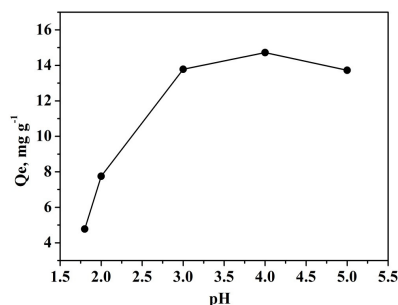
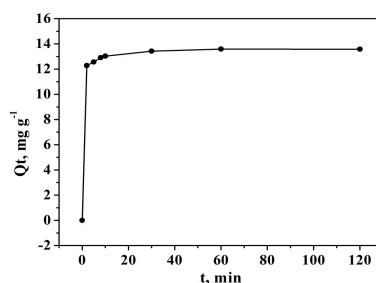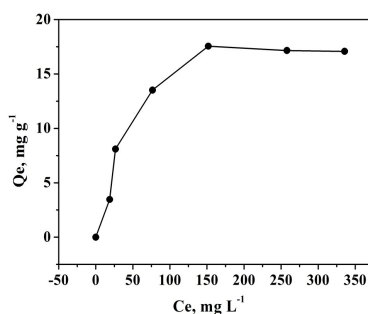Figure 4: Adsorption efficiency of HP as a function of initial solution pH

Figure 5: Effect of contact time on Cu^{2+} adsorption onto HP

Figure 6: Experimental adsorption isotherm for HP

Effect of contact time

The effect of contact time was studied at pH 4.0 and initial Cu^{2+} concentration of 200 mg L^{-1}. Figure 5 shows the dependence of contact time on the adsorption capacity Q_e (mg g^{-1}) of Cu^{2+} ions for HP. It was observed that the adsorption capacity increased rapidly with increasing agitation time and reached equilibrium after 12 min, which shows a very fast adsorption rate. The short time for reaching equilibrium indicates that the biosorbent has high affinity towards Cu^{2+} ions.

Adsorption isotherms

The adsorption isotherm describes the distribution of the adsorbed species between the liquid and solid phases in equilibrium state. The elucidation of isotherm data by fitting them to different isotherm models is a substantial step in the adsorption study. The experimental isotherm of the investigated material is presented in Figure 6.

The adsorption data were also analyzed with the linearized forms of Langmuir, Freundlich and Dubinin–Radushkevich isotherm models.[5]

Langmuir isotherm

The linear form of the Langmuir isotherm is expressed by the following equation:

$$C_e/Q_e = 1/K_L Q_0 + C_e/Q_0 \qquad (2)$$

where C_e is the concentration of metalions in the equilibrium solution (mg L^{-1}), Q_e is the amount of ion adsorbed (mg) per unit mass of adsorbent (g), Q_0, the maximum adsorption capacity (mg g^{-1}); K_L is the Langmuir constant related to enthalpy of the process.

The Langmuir model supports the following hypothesis: the adsorbent has a uniform surface – absence of interactions between solid molecules; the sorption process takes place in a single layer.

Freundlich isotherm

The linear form of the Freundlich model is expressed by the following equation:

$$lnQ_e = lnk_F + (1/n) \, lnC_e \qquad (3)$$

where k_F is a constant related to the adsorption capacity and n is an empirical parameter related to the intensity of adsorption.

The Freundlich model is valid for heterogeneous surfaces and predicts an increase in the concentration of the ionic species adsorbed onto the surface of the solid when increasing the concentration of certain species in the liquid phase.

Dubinin–Radushkevich isotherm

The Dubinin–Radushkevich isotherm reveals the adsorption mechanism based on the potential theory. The linear form of the Dubinin–

Radushkevich isotherm is described by the following equation:

$$lnQ_e = lnQ_m - \beta\varepsilon^2 \tag{4}$$

where Q_e is the amount of metal ion (mg) adsorbed per unit mass of adsorbent (g), Q_m is the maximum adsorption capacity (mg/g), β is the adsorption energy constant (mol^2 J^{-2}), and ε is the Polanyi potential, described as:

$$\varepsilon = RT\,ln(1+1/C_e) \tag{5}$$

where R is the gas constant (J mol^{-1}K^{-1}) and T is the temperature (K). The mean adsorption energy E (KJ mol^{-1}) can be calculated using the parameter β as follows:

$$E = 1/(-2\beta)^{1/2} \tag{6}$$

The calculated isotherm constants and the correlation coefficients for the three models discussed above are presented in Table 1. From the correlation coefficient r^2 (greater than 0.95), it is clear that both Langmuir and Dubinin–Radushkevich models are adequate in describing the adsorption processes. The linear fit to the Langmuir model is not as good for the investigated material, as compared to that to the Dubinin–Radushkevich model (correlation coefficients r^2 0.9564 for Langmuir and 0.9858 for Dubinin–Radushkevich model, respectively). As the coefficient of correlation r^2 for the Dubinin–

Radushkevich model is the highest from all the models applied and the saturation/maximum capacity seems to be reached (Fig. 6), the equilibrium adsorption capacity was calculated from the Dubinin–Radushkevich isotherm model and it was found to be 16.94 mg g^{-1} for HP. This adsorption capacity is compared with those reported in the literature[10,17-22] (Table 2). It is evident that the material HP displays reasonably good adsorption capacity for Cu(II) and it could be used as potential adsorbent for the effective removal of these ions from contaminated aqueous solutions. The Dubinin–Radushkevich isotherm model gives information about the adsorption energy. The calculated mean free energy E is 0.07 kJ mol^{-1} for HP, indicating mainly a physisorption process.

SEM analysis

SEM was used for the characterization of the morphology and structure of the HP biosorbent before and after Cu^{2+} adsorption. The SEM micrograph of the initial material (Fig. 7 (a)) indicates that the biomass has rough and heterogeneous morphology, containing a large number of pores of different size, which enables the sorption of various metal ions into the different parts of the biosorbent.

Table 1

Isotherm constants and correlation coefficients for the three models for Cu^{2+} adsorption onto HP

Langmuir parameters			Freundlich parameters			Dubinin-Radushkevich parameters		
Q_0 (mg g^{-1})	K_1 (L mg^{-1})	r^2	k_F (mg^{1-n}L^n g^{-1})	n (L mg^{-1})	r^2	$Q_{m(0)}$ (mg g^{-1})	E (kJ mol^{-1})	r^2
20.67	0.019	0.9564	1.24	2.03	0.7597	16.94	0.07	0.9858

Table 2

Comparison of adsorption capacities with respect to Cu(II) ions in the present study with those reported in the literature

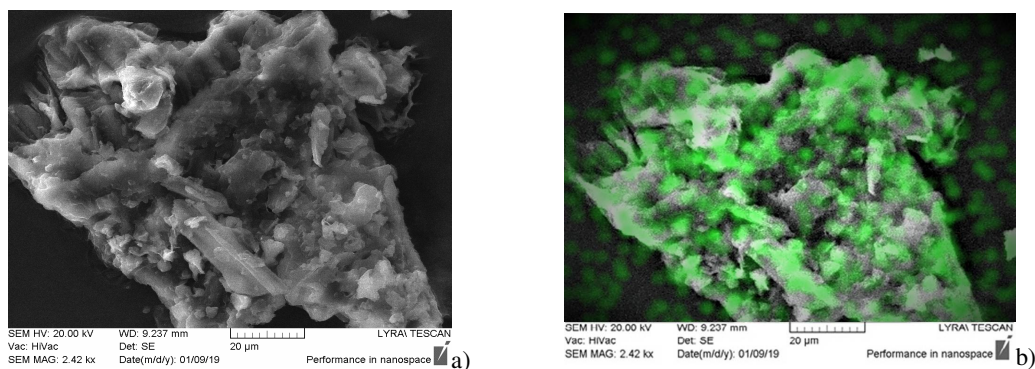| Biosorbent	q_{max} (mg/g)	Reference
Rape straw powders	32.00-70.06	Liu et al.[10]
Eichhornia crassipes	22.7	Zheng et al.[17]
Persimmon leaves	19.42	Lee et al.[18]
Amaranthus spinosus L.	13.1	Chen et al.[19]
Chestnut shell	12.56	Yao et al.[20]
Lagenaria vulgaris shell	12.15	Stanković et al.[21]
Solanum nigrum L.	9.68	Chen et al.[19]
Sugarcane bagasse	9.48	Liu et al.[22]
Banana peels	8.24	Liu et al.[22]
Watermelon rind	5.73	Liu et al.[22]
Hypericum perforatum L.	16.94	Present study

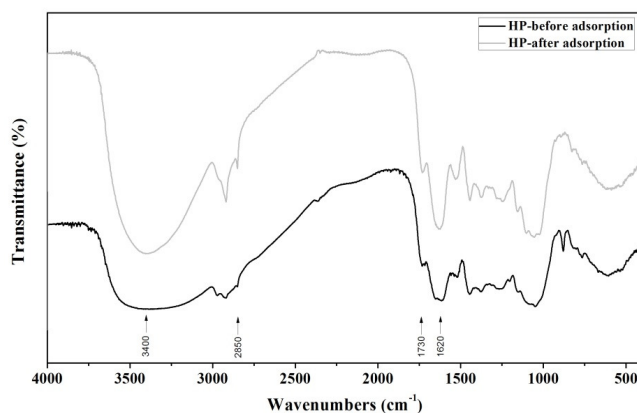Figure 7: Scanning electron micrographs of the surface of HP before (a) and after (b) Cu^{2+} adsorption

Figure 8: FTIR spectra of HP before and after Cu^{2+}adsorption

The SEM micrograph of the HP biosorbent loaded with copper is shown in Figure 7 (b). The porous cavities occupied by the adsorbed copper are visible as dots on the SEM image. As can be seen, the adsorbed copper ions are distributed homogenously on the biosorbent surface.

FTIR analysis

The plant materials mainly consist of cellulose, hemicellulose and lignin. They contain many functional groups, such as hydroxyl, carbonyl, carboxyl and amino groups, with characteristic chemical structures. To determine the surface functional groups responsible for the adsorption properties of the studied plant, the FTIR spectra before and after Cu^{2+} adsorption in the range of 4000-400 cm^{-1} were recorded and shown in Figure 8, and the bands where significant shifting is observed, are presented in Table 3.

A very broad band between 3700 and 3000 cm^{-1} is attributed to the stretching vibrations of the multitude of the hydroxyl groups in phenolic and aliphatic structures, also aromatic and aliphatic NH groups, all influenced by hydrogen bonding and overlapped by stretching vibrations of water molecules. The group of bands around 2850 cm^{-1} belongs to the asymmetric and symmetric stretching C-H vibrations in methoxyl, methyl, methylene and methylylidene groups in the side chains of aromatic and aliphatic structures. The bands and shoulders observed around 1730 cm^{-1} were attributed to carbonyl groups from the structures of ketones, aldehydes, esters, acids, *etc*. The intensive band around 1620 cm^{-1} is the result of contributions from the stretching modes of C=C double bonds (isolated and conjugated), ring-conjugated C=O bonds and C−O bonds in carboxylate groups.[23,24]

Looking at the spectra, band shifting and possible involvement of hydroxyl and/or amino groups around the broad peak at 3400 cm^{-1} may be noticed. The peak at about 2850 cm^{-1} is also shifted. Little change is observed in the carboxyl band at 1738 cm^{-1} and an increase in the asymmetric C=O band at 1614 cm^{-1} indicates some carboxyl binding. If the shift is less than instrument resolution (4 cm^{-1}), it is not taken into account and cannot be discussed reliably. From the spectra, it appears that carboxyl, hydroxyl and

amino groups are involved in Cu binding to the HP, which is in accordance with Khormaei et al.[24] Probably, this plant contains components with functional groups, which are readily available for coordination. The involvement of functional groups, containing hydrogen and oxygen atoms in the adsorption of Cu(II) ions is a proof that the process of copper retaining is a combination of ion exchange and surface complexation, which is in accordance with the findings of the pH study.

Table 3
FTIR results showing the bands with significant shifting after Cu^{2+} adsorption on HP
(wavenumbers presented in cm^{-1})

Sample	-OH and –NH groups	CH, CH_2 and CH_3 groups	C=O from carboxylic, ester etc. groups	C=C,C=O and C−O bonds
HP before adsorption	3365	2853	1738	1614
HP after adsorption	3408	2845	1730	1626

Desorption studies

The Cu^{2+} ions adsorbed onto the investigated biosorbent were eluted with 0.1M HNO_3, 1M HNO_3 and 0.1M EDTA. Diluted HNO_3 could not be used for desorption of Cu^{2+} ions (about 50% desorption). Both eluting agents 1M HNO_3 and 0.1M EDTA showed higher, almost equal recovery efficiency, more than 95%.

CONCLUSION

The adsorption properties of a material based on Hypericum perforatum L. (denoted as HP) towards Cu^{2+} ions was investigated. XRD patterns revealed peaks of cellulose I and amorphous phase due to lignin, hemicelluloses and amorphous cellulose. TGA plots showed four regions, corresponding to the elimination of moisture and adsorbed water from the sample and thermal decomposition of hemicelluloses, cellulose and lignin. The FTIR spectra of HP before and after adsorption indicated that carboxyl, hydroxyl and amino groups were involved in Cu(II) binding.

SEM analysis after metal loading revealed that the copper ions were distributed homogenously on the biosorbent surface. The linear Langmuir, Freundlich and Dubinin–Radushkevich models were used to analyze equilibrium experimental data and it was established that the Dubinin–Radushkevich isotherm most adequately described the adsorption process. The maximum adsorption capacity was found to be 16.94 mg g^{-1}, which proved the good potential of the investigated material as a biosorbent for the removal of copper ions from aqueous solutions.

REFERENCES

[1] D. Sud, G. Mahajan and M. P. Kaur, Bioresour. Technol., **99**, 6017 (2008), https://doi.org/10.1016/j.biortech.2007.11.064
[2] J. A. Laszlo and F. R. Dintzis, J. Appl. Polym. Sci., **52**, 531 (1994), https://doi.org/10.1002/app.1994.070520408
[3] E. Pehlivan, T. Altun and S. Parlayıcı, J. Hazard. Mater., **164**, 982 (2009), https://doi.org/10.1016/j.jhazmat.2008.08.115
[4] B. Volesky, Hydrometallurgy, **59**, 203 (2001), https://doi.org/10.1016/S0304-386X(00)00160-2
[5] P. S. Vassileva, A. K. Detcheva, T. H. R. Radoykova, I. A. Avramova, K. I. Aleksieva et al., Cellulose Chem. Technol., **52**, 633 (2018), https://www.cellulosechemtechnol.ro/pdf/CCT7-8(2018)/p.633-643.pdf
[6] B. M. W. P. K. Amarasinghe and R. A. Williams, Chem. Eng. J., **132**, 299 (2007), https://doi.org/10.1016/j.cej.2007.01.016
[7] A. Gundogdu, D. Ozdes, C. Duran, V. N. Bulut, M. Soylak et al., Chem. Eng. J., **153**, 62 (2009), https://doi.org/10.1016/j.cej.2009.06.017
[8] A. Dubey and A. Mishra, J. Renew. Mater., **5**, 54 (2017), https://doi.org/10.7569/JRM.2016.634127
[9] S. Stoyanov, "Heavy Metals in the Environment and Nutrient Products; Toxic Effects on Humans; Clinical Picture, Treatment and Prophylaxis", Pensoft, Sofia, 1999, pp.5 (in Bulgarian)
[10] X. Liu, Z.-Q. Chen, B. Han, C.-L. Su, Q. Han et al., Ecotox. Environ. Safe., **150**, 251 (2018), https://doi.org/10.1016/j.ecoenv.2017.12.042
[11] C. S. T. Araujo, I. L. S. Almeida, H. C. Rezende, S. M. L. O. Marcionilio, J. J. L. Leon et al., Microchem. J., **137**, 348 (2018), https://doi.org/10.1016/j.microc.2017.11.009
[12] S. Park, J. O. Baker, M. E. Himmel, P. A. Parilla and D. K Johnson, Biotechnol. Biofuels, **3**, Article

number 10 (2010), https://doi.org/10.1186/1754-6834-3-10

[13] C. Hongzhang, "Biotechnology of Lignocellulose: Theory and Pratice", Springer, London, 2014, pp. 25-71, https://www.springer.com/gp/book/9789400768970

[14] G. Yuvaraja, N. Krishnaiah, M. V. Subbaiah and A. Krishnaiah, *Colloid. Surface. B*, **114**, 75 (2014), https://doi.org/10.1016/j.colsurfb.2013.09.039

[15] D. Ciolacu, F. Ciolacu and V. I. Popa, *Cellulose Chem. Technol.*, **45**, 13 (2011), https://www.cellulosechemtechnol.ro/pdf/CCT1-2(2011)/p.13-21.pdf

[16] V. B. Shinde and M. Singarvelu, *J. Environ. Res. Develop.*, **9**, 151 (2014), http://www.jerad.org/archiveabstract.php?vol=9&issue=1

[17] J.-C. Zheng, H.-M. Feng, M. H.-W. Lam, P. K.-S. Lam, Y.-W. Ding *et al.*, *J. Hazard. Mater.*, **171**, 780 (2009), https://doi.org/10.1016/j.jhazmat.2009.06.078

[18] S.-Y. Lee and H.-J. Choi, *J. Environ. Manag.*, **209**, 382 (2018), https://doi.org/10.1016/j.jenvman.2017.12.080

[19] J.-P. Chen, W.-R. Chen and R.-C. Hsu, *J. Ferment. Bioeng.*, **81**, 458 (1996), https://doi.org/10.1016/0922-338X(96)85148-8

[20] Z.-Y. Yao, J.-H. Qi and L.-H. Wang, *J. Hazard. Mater.*, **174**, 137 (2010), https://doi.org/10.1016/j.jhazmat.2009.09.027

[21] M. N. Stanković, N. S. Krstić, J. Z. Mitrović, S. M. Najdanović, M. M. Petrović *et al.*, *New J. Chem.*, **40**, 2126 (2016), https://doi.org/10.1039/c5nj02408k

[22] C. Liu, H. H. Ngo, W. Guo and K.-L. Tung, *Bioresour. Technol.*, **119**, 349 (2012), https://doi.org/10.1016/j.biortech.2012.06.004

[23] M. Jarzębski, W. Smułek, H. M. Baranowska, Ł. Masewicz, J. Kobus-Cisowska *et al.*, *Food Hydrocolloid.*, **104**, Article number 105748 (2020), https://doi.org/10.1016/j.foodhyd.2020.105748

[24] M. Khormaei, B. Nasernejad, M. Edrisi and T. Eslamzadeh, *J. Hazard. Mater.*, **149**, 269 (2007), https://doi.org/10.1016/j.jhazmat.2007.03.074